ISSN XXXX XXXX © 2019 IJESC

Research Article Volume 9 Issue No.3

IoT Based Air Ambulance

S. Jeevitha[1], P. Gomathi[2], C. Divya[3], Mr. M. Vedaraj[4]
Department of Computer Science and Engineering
R.M.D. Engineering College, Chennai, Anna University, Tamil Nadu, India

Abstract:
Wireless all-analog biosensor style for the simultaneous microfluidic and physiological signal observance is conferred in this paper. The key part is associate degree all-analog circuit capable of pressure 2 analog sources into one analog signal by the analog joint source-channel cryptography (AJSCC). 2 circuit designs are mentioned, together with the stacked-voltage-controlled voltage supply (VCVS) style with the mounted variety of levels, and an improved style, that supports a versatile variety of AJSCC levels. Experimental results are conferred on the wireless biosensor prototype, composed of computer circuit board realizations of the stacked-VCVS style. what is more, circuit simulation and wireless link simulation results are conferred on the improved style. indicate that the planned wireless biosensor is compatible for sensing 2 biological signals at the same time with high accuracy, and can be applied to awide style of low-power and affordable wireless continuous health observance applications.

Index terms: Analog Compression, Microfluidic Sensing, Physiological Signal Sensing, Wireless Sensors.

1. INTRODUCTION

The design of wireless biosensors is crucial to the belief of wireless health watching solutions [2]. Wireless monitoring of physiological signals brings the benefits of movableness [3], wearability [4], continuous measurements [5], and improved point-of-care to patient compared with wired counterparts. what is more, microfluidic biosensor shave emerged as powerful tools for wearable biomarker watching, including electrical resistance detection [6], large Magneto resistance (GMR) sensing [7], and chemical science detection [8], [9]. Microfluidic sensing will change wearable sensors that are minimally invasive thanks to the minute sample volumes needed for correct sensing, so promoting customized health monitoring through continuous quantification of biomarkers. The detection of assorted biomolecules in blood samples mistreatment impedance-based bio-detection has been incontestable in previous works [10], that shows the potential to comprehend really miniaturized wearable diagnostic platforms. Among the microfluidic sensors, impedance-based sensors usually integrate electrodes in microfluidic channels and monitor changes in resistivity as particles flow over the electrodes. This category of sensors has been shown to be suited to police work biomarkers with high sensitivity [11], [12]. Impedance-based sensors are often created portable with miniaturized analog front-end electronic equipment like lock-in-amplifiers [13], and wireless transmitters. Functionalization of microfluidic channels in resistivity cytometers with different types of antibodies and enzymes will change biomarker detection with high specificity. There are varied situations wherever a network of wireless body sensors observance each physiological signals and molecular biomarker concentrations are useful to patient care. One medical state of affairs is observance hospitalized patients with cardiovascular unwellness. there's an unlimited body of literature concerning the benefits of observance patients with vas disease incessantly. Kario et al. [14] incontestible the usage of wireless sensors to observe the physiological signals of blood pressure and also the environmental parameters for patients with cardiovascular unwellness. Hu et al. [15] conferred a microfluidic based portable device to boost point-of-care observance of cardiovascular disease patients. we have a tendency to envision wireless wearable sensors probably replacement wired tags accustomed monitor physiological signals together with graph (ECG), heart rate, rate of respiration, vital sign, temperature and blood oxygen levels by electrical or optical sensors, providing continuous wireless observance of those important signs. additionally, various blood biomarkers reflective the state of the vas and system, also can be monitored in these wearable sensing element networks. Potential internal organ markers of interest include levels of internal organ Troponin, BNP, creatinine, C-reactive protein (CRP), and conjointly complete somatic cell counts. The true power of each physiological and biomarker measurements will be realised once each are combined along and also the correlations between the 2 information sorts are higher understood. In this work, we have a tendency to gift a wireless biosensor style that may live physiological signal and molecular biomarkers at the same time. A network of body sensors observance varied physiological parameters simultaneously with biomarker observance in blood, sweat, and exhaled breath condensation will greatly improve our understanding of unwellness pathological process. Manuscript received Gregorian calendar month four, 2017; revised Jan four, 2018 and March eight,2018; accepted March nine, 2018. Date of publication May twenty-nine, 2018; date of current version Gregorian calendar month five, 2018. This paper was conferred partially at the IEEE International Symposium on Circuits & Systems, Baltimore, MD, USA, could 2017 [1]. This paper was counseled by Associate Editor M. Kalofonou. (Corresponding author: Vidyasagarsaddhu.) The authors are with the Department of Electrical and pc Engineering, Rutgers University, New Brunswick, NJ 08901-8554 USA(e-mail:, xueyuan.zhao@rutgers.edu; vidyasagar.sadhu@rutgers.edu; tuananh.le@rutgers.edu; pompili@rutgers.edu; mehdi. Javan mard @rutgers.edu).Color versions of 1 or additional of the figures during this paper are obtainable on-lineat http:// ieeexplore.ieee.org. Digital Object symbol ten.1109/ TBCAS. 2018. 2829512 The circuit style of the biosensor forms the muse of this kind of hybrid wearable wireless biosensing platform. Existing wireless biosensor styles depend upon digital circuits that have high complexness and are power inefficient. These limitations hinder a lot of required options of large-scale deployment and battery-less watching. during this

work, we are bridging the technological gap between hybrid detector style and analog electronic equipment, by introducing a selected sort of analog signal compression circuit that's geared toward press microfluidic and physiological signals, while not the necessity of digital circuits. This work ultimately eliminates the operations of conversions between digital and analog signals, so considerably improving the ability potency of biosensor circuits. Moreover, signal recovery performance of the projected circuit is guaranteed for target applications.

Existing Work:
A sensing system was incontestible [16] where sweat-lactate concentration is measured electrochemically with a co-occurring ECG activity. Here, the sweat lactate concentration Associate in Nursing ECG signals are 1st passed to an Analog-to-Digital Converter (ADC) for process by a microcontroller, and so are wirelessly transmitted via Bluetooth module. Luhmann et al. [17] incontestible a wireless sensing element that at the same time measures the graph and neuroscience signal exploitation digital transmission of the info via Bluetooth. Abrar et al. [18] conferred a wireless sensing element during which the sweat lactate is measured and therefore the sensing signal is sampled with Associate in Nursing ADC, processed by a chip, and so transmitted by a digital Near-Field Communication (NFC) wireless module. Nemiroski et al. [19] designed a digital mobile system for the transmission of chemistry detection knowledge. all told these systems, the main power consumption is because of the digital conversion by the ADCs and ulterior process by the microcontrollers, that limits the battery lifetime of the devices and the usefulness of the system. Our previous work [20] projected an Associate in Nursingalog compression circuit for 2 signals, and introduces the technique during a generalizable context. However, it had been restricted to wireless circuits solely and didn't embrace biosensors for biomarker detection, that involves measurement signals that are rapidly ever-changing, so the challenges involved the present manuscript are of a special nature, and need vital testing and integration of a replacement form of readout circuit, namely the lock-in-amplifier. within the current manuscript, we have a tendency to are integration two sensors that are of a special category and fully different nature, a physiological signal sensing element that is a lot of of a physical activity, and a microfluidic electric resistance sensing element, which falls below the category of biological/chemical measurements. In this manuscript, we, for the primary time ever, show the potential for exploitation Analog Signal compression for signals obtained from these 2 completely different categories of signals. For this purpose, we have a tendency to performed novel experiments to attain coincident microfluidic impedance cytometry and physiological signal sensing. We also performed systematic wireless link level simulations to gauge the signal recovery performance of the projected wireless biosensing system below varied indoor and out of doors signal propagation conditions. This work shows the promise of our vision for a compression theme that will work with a network of body sensors that are unceasingly getting each physical and organic chemistry knowledge.

Our Contributions: During this study, we tend to mimic the activity of blood cells on a microfluidic electrical phenomenon cytometer (microfluidic channel with thirty µm dimension and twenty µm height) exploitation 7.8 µm diameter beads in saline buffer. The physiological signals are the electrical Galvanic Skin Response (GSR) activity of skin electrical phenomenon via Shimmer sensors with a most worth of 2.6 Ω−1. This work is distinct from previous works therein the detected physiological and biomarker analog signals are directly compressed within the associate degreealog domain by an analog circuit, and are modulated and transmitted via analog oftenness (RF) communication chain. There are not any power-hungry digital circuits like ADCs, Digital-to-Analog Converters (DACs) or microprocessors within the sensing element that permits the sensing element to run on power gathered from energy-harvesting techniques like human motion. The all-analog circuit performing arts the compression relies on associate degree cryptography technique termed Analog Joint Source Channel secret writing (AJSCC) [21]–[23], wherever a digital Cluster Head (CH) receiver performs the AJSCC cryptography to recover the supply signals. the main contributions of this work include: associate degree all-analog wireless biosensor style is conferred, consisting of synchronous microfluidic electrical phenomenon sensing as well as physiological signal sensing and resulting signal compression by associate degree AJSCC circuit. 2 circuit styles of the AJSCC cryptography are presented—the initial supporting a hard and fast and tiny range of AJSCC levels, and therefore the second supporting a versatile and larger range of levels (within a particular range). The conferred biosensor system is valid via hardware experiments exploitation the primary style (Design 1), and by circuit and wireless link simulations for the second style (Design 2).

Article Outline: In Section II, our wireless biosensor style for twin measurements is conferred as well as its equivalent circuit model, microfluidic device fabrication procedure, and improved style for AJSCC cr

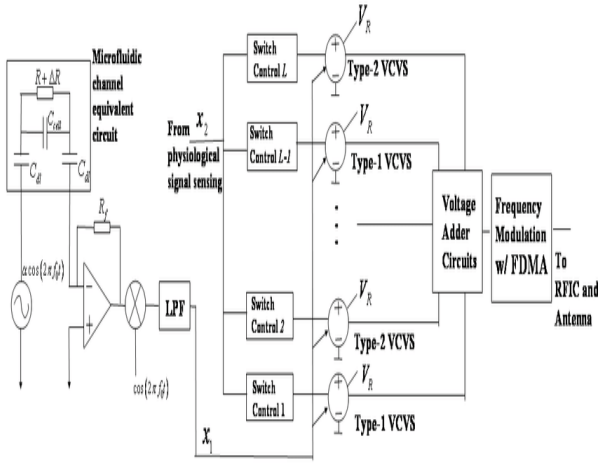

yptography electronic equipment. In Section III, hardware experimental results for style one, circuit simulation and wireless link simulation results for style a pair of are conferred. Finally, in Section IV, conclusions are drawn.

II.PROPOSED WIRELESS BIOSENSOR PROTOTYPE

We initial gift the system style of the wireless biosensor prototype together with the equivalent circuit model of the microfluidic channel, the paradigm system setup, and also the microfluidic device fabrication procedure in Section II-A. Then, Associate in Nursing improved circuit style of the AJSCC coding, Design 2, is bestowed in Section II-B.

A. Wireless sensing element System
The wireless sensing element circuit portrayed in Fig. 1, consists of the microfluidic sensing circuit, and also the all-analog signal compression and wireless transmission circuits.

The microfluidic system adopts impedance-based particle-concentration measure. The equivalent circuit of the impedance-based microfluidic system during this study has been used for previous work alsoin [24]. The microfluidic device consists of the microfluidic PDMS (poly dimethy lsiloxane) channel on a try of co-planar electrodes. The equivalent circuit within the microfluidic channel and the sensing element will be shapely by 2 double-layer capacitors Cdl, one resistance R, and one condenser Ccell in parallel as shown in Fig. 1. once a molecule passes by, the resistance can have an amendment in resistance ΔR, which is able to end in an amendment in signal detection. The electrical phenomenon measure is happy with a trigonometric function wave with frequency f0. The resistance amendment ΔR and the voltage amendment are detected and amplified by the lock-in electronic equipment with feedback resistance Rf. The signal is then passed to a mixer with frequency f0 and so through a lowpass filter. For this equivalent circuit model, molecules passing the conductor can cause electrical phenomenon variation, and molecules of different sizes can have completely different electrical phenomenon variation within the output pulse response. The sensitivity depends on variety of conditions, together with the scale of the microfluidic channel, the selection of the excitation frequency, the background level of the front-end circuit, and also the detection algorithmic rule. Associate in Nursing optimized impedance-based microfluidic system considering all of those parameters will sight sub-µm particles. In our previous work, we have shown that the microfluidic sensing element will sight micronsized beads variations at intervals two µm in diameter (adequate for cells). In different studies, researchers have incontestible the flexibility to sight particles at the nano-scale [25], [26].

System Setup: To demonstrate a proof-of-concept style, we quantify the microbeads within the microfluidic channel to mimic the blood cell quantification method. during this work, the sensing element quantifies the quantity of beads, that is analogous to however the quantity of cells during a blood sample would be quantified. The detection of real cells during a advanced biological sample like blood is on the far side the scope of this work. The cells are loaded into the micro-channel and directed to the microfluidic sensing region. The particles passing the conductor can manufacture pulses within the voltage output as represented in [10], [24]. The microfluidic signal is generated by micron-sized beads passing through the co-planar conductor pair within the microfluidic channel with a dimension of thirty µm and a height of twenty µm. The conductor dimension is twenty µm dimension and 200 nm length, with a spacing of twenty-five µm between the conductor pair. The effective length of the electrodes is thirty µm, which is the amount overlapping with the microfluidic channel and is exposed to the solution. The signal is happy with cosine-ware frequency f0 of five hundred kilocycles per second. The rate of flow is zero.1 µL/min. The bead size is 7.8 µm. A sequence of pulses is generated with beads flowing over the conductor try and also the signal is recovered mistreatment the lock-in electronic equipment analog circuit [13].

Microfluidic sensing element Fabrication:
The microfluidic electrical phenomenon cytometer is fancied mistreatment soft lithography [27]. The sensing element and also the microchannel are fancied one by one before incorporating into the microfluidic device. Photomasks for the lithography processes are designed mistreatment AutoCAD. The photomasks are fancied by Advance Reproductions corporation. (North Andover, MA).

i) Microfluidic Channel: The microchannel is built mistreatment PDMS and commonplace molding techniques [27]. The master mold is fancied with SU-8 photoresist. To fabricate the microchannel, PDMS answer is poured onto the mould and cured at eighty ◦C for Associate in Nursing hour. when solidifying, the PDMS is in the altogether removed from the mould to make the microfluidic channel.

ii) Microelectrode: The microelectrodes are fancied on the glass substrate mistreatment commonplace lithography. Photoresist AZ5214 is spin coated on the substrate and exposed to UV light beneath the microelectrode photomask. The coated glass wafer is then developed in AZ5214 developer. The photoresist exposed to UV light would be washed away making the pattern of the microelectrodes. a skinny layer of Cr and gold (50 A˚ and two hundred nm respectively) are deposited on the wafer mistreatment using electron beam evaporation.

iii) Microfluidic Device: A PDMS chip embedded with a microchannel is covalently secure to the glass wafer with microelectrodes to make the microfluidic device. The surfaces of glass and PDMS are exposed to chemical element plasma to get thin layers of silanol terminations (SiOH). once brought in contact with the modify glass surface, the silanol terminated layers close to make the conformal Si-O-Si valency bonds between the chemical compound and glass [28]. The chemical element plasma 464 I also make the PDMS surface deliquescent [29]. this permits for capillary flow of fluid/cells through the resistivity cytometer without the necessity for external syringe pumps.

Key detector Circuit style 1: The circuit design (Design 1) of the AJSCC secret writing is portrayed in Fig. 1. within the all-analog realization of AJSCC circuit [21], the microfluidic sensing signal x1 controls the output of Voltage Controlled Voltage Sources (VCVS). Note that there are 2 varieties of VCVS, type-1 and type-2. For type-1 VCVS, the output voltage of VCVS will increase linearly with the increment of the dominant voltage x1 , which corresponds to the odd-numbered levels in AJSCC; and for type-2 VCVS, the output voltage of VCVS decreases linearly with the increment of the dominant voltage x1 , that corresponds to the even-numbered levels in AJSCC. every VCVS is switched among saturation voltage VR, the linear voltage output resembling x1, and ground. The physiological signal x2 is that the management signal of the VCVS composed of L stages. With larger physiological signal, there'll be additional stages being activated. as an example, if there are M stages being activated, the M-th stage are controlled by the signal returning from the impedance cytometer x1 to provide never-ending variable output voltage, and also the first to the M − 1th stages can output the utmost voltage VR. the opposite higher L − M stages turn out zero grounded outputs. The voltages of all the stages are summed together by associate degree analog voltage adder to provide the required AJSCC encoded voltage. The signal is then passed to RFIC and the antenna. thanks to the stacking of multiple VCVS blocks resembling totally different stages, we tend to decision this “Stacked VCVS” style. The power consumption of our analog AJSCC board (with “Stacked VCVS” design) while not radio power is calculable to be a hundred thirty µW for a discrete-component realization as follows [21]. Our circuit in total (5 and a [*fr1] stages/11 levels) consists of sixteen OpAmps, seventeen Comparators, and eleven Multiplexers, where OpAmps are clearly the key contributors to the general power consumption. There are

several low-power styles planned for these parts. as an example, a low-power OpAmp [30] consuming concerning eight μW, a comparator [31] overwhelming concerning 12.7 nW, associate degreed an analog electronic device (ADG704) overwhelming about ten northwest are often used for our circuit leading to an influence consumption of a hundred thirty μW. we tend to believe this variety are often even lower (to but fifty μW) if an computer circuit (IC) style is adopted, thanks to the subsequent reasons: (i) a style victimisation discrete parts for various functionalities of the circuit uses further hardware as inter-component improvement isn't possible as in associate degree IC implementation; (ii) generally, the larger the area of the chip, the upper the facility consumption [32], which is thanks to the employment of a bigger substrate or a mixture of many smaller substrates (corresponding to totally different separate components). On the opposite hand, in an IC, all the functionalities are designed on prime of one little substrate leading to a lot of lower area and, hence, a way lower power consumption; (iii) victimisation IC style permits the employment of latest nm-Si (nanometer-Silicon) technology (e.g., ten nm presently or five nm in close to future) for the fabrication of the chip, that once more leads to lower power consumption because the space is reduced attributable to lower dimensions of the transistors' channel. we tend to expect these reasons can facilitate reduce the facility consumption by over [*fr1] leading to B.

Key detector Circuit style 2:

There is a scope of any reduction in power consumption and circuit quality (which interprets to cost) of the AJSCC circuit in style one (Section II-A). As are often detected, Design 1 adopts a set range of AJSCC levels that has to be set before the fabrication of the chip, creating the sensing resolution in x2 fastened once the chip is unreal. On the opposite hand, it may be necessary to vary the sensing resolution supported the application. as an example, till sure symptoms are detected a lower resolution in x2 (i.e., higher Δ) are often adopted and therefore the resolution is often augmented if some preliminary symptoms are detected. Secondly, in style one, the hardware reminiscent of each level/stage is duplicated as over and over because the range of AJSCC levels. this can be associate inefficient approach, each in terms of power consumption moreover as complexity/cost because the hardware in every level are often reused rather than being duplicated. Finally, since having an oversized range of AJSCC levels is tedious with this approach (since it doesn't scale well with the quantity of levels), it results in a lot of quantisation in x2 (as are often ascertained in the experimental section, Section III-A). In order to deal with the on top of limitations of style one, we present a unique style two wherever the quantity of AJSCC levels will be user outlined among a particular vary (even once the fabrication of the chip) moreover as has abundant lower power consumption and circuit quality compared to style one (especially for range of levels larger than 16). The improved detector circuit style (Design 2) is given in our previous work [20]. To connect this circuit with biosensing, the physiological signal x2 is initial divided by the tuneable spacing between levels, Δ employing a period of time analog divider to supply the quotient of the division. The quotient is fed to 2 blocks—an associate log number and an odd/even detector block that detects whether or not the quotient is odd or maybe. On the opposite hand, the microfluidic signal, x1 is fed to each type-1 VCVS and type-2 VCVS blocks to supply respective type-1 or type-2 outputs that are proportional and inversely proportional to x1 severally. whether or not to use type-1 output or type-2 output depends on that numbered level the mapped AJSCC purpose is (where the quantity is that the quotient of the division). If it falls on an excellent level (0, 2,), type-1 output needs to be thought of and vice-versa. Hence, the odd/even detector (of quotient) will management that output is taken into account via associate analog switch. Then the quotient increased by the extent saturation voltage, VR is superimposed to the switch output to supply the final AJSCC encoded voltage. We have enforced the whole encryption circuit of style two, i.e., from inputs x1 and x2 until the output of adder victimization Spice [20], where, the multi-stage analog divider and odd/even detector block combined are enforced as one circuit. For further details on the implementation, comparison with style one in terms of complexness and power consumption, most and minimum variation in Δ (in different words, the amount of levels, L) supported by the circuit, please consult with our previous work [20]. the selection of the parameter L, depends on the distribution of the supply signals, the transceiver style, and the wireless channel conditions. to seek out the best parameter L, we need to gauge the wireless communication system performance below completely different channel conditions, that has been done in Section III-B. From these results, we have a tendency to are ready to build the judgment on the best L for a given biosensing application. In this section, we tend to gift the validation results of the projected biosensing platform. Specifically, we tend to gift the experimental results of our wireless biosensor exploitation the AJSCC Printed Circuit Board (PCB) implementation of style one in Section III-A. Then, the circuit simulation results of style two and wireless link simulation results of the device with style two to find the optimum parameters are given in Section III-B.

A. Experimental Results with style 1:

The experiment is intended as a signal of thought to verify the functionalities of the key device circuit style one (11 AJSCC levels exploitation stacked VCVS design) at the transmitter aspect as well as at the receiver to recover the 2 compressed signals.

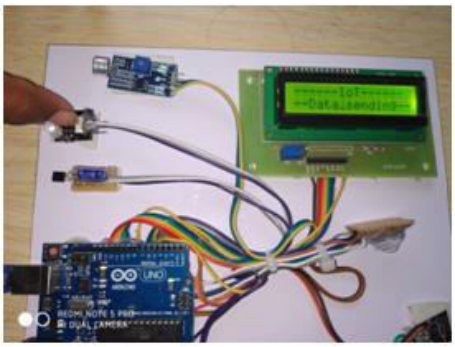

Experimental Setup: The take a look at is performed in an interior setting with a carrier frequency of two.4 gigacycle per second and an antenna. the space between the transmitter and receiver is regarding five meters. The transmitter system is shown in Fig. 2. The physiological signal is chosen to be an electrical skin response signal connected via Bluetooth exploitation Shimmer sensors, and also the signal is regenerated exploitation metallic element LabView/DAQ system. each of those signals are fed to the board developed in [21] to perform the device signal coding within the anal Transmitter AJSCC Encoding: the first microfluidic signal, physiological signal, and therefore the AJSCC encoded signal within the transmitter are delineated in Fig. 3(a) as captured mistreatment Ni DAQ hardware and LabView computer code. We can observe that AJSCC coding compresses the 2 signals into one specified the microfluidic signal is riding on prime of

the physiological signal. we tend to note that our AJSCC sensor board introduces a division error within the physiological signal since it's solely eleven levels within the y-dimension, as seen in Fig. 3(a) wherever the physiological signal portion within the AJSCC encoded signal has been measure. This AJSCC encoded signal is frequency modulated, upconverted, and so transmitted mistreatment Commercial Off the Shelf (COTS) RFIC chip. Receiver Decoding: At the receiver, the signal is down converted (to baseband) and so frequency demodulated to recover the AJSCC encoded signal. The reception method is as follows. The baseband signal is captured into LabView using associate Ni DAQ device. Then the signal is foremost sampled with a rate fs, then the frequency of the signal is detected by associate quick Fourier remodel (FFT)-based frequency detector with Ns samples per FFT. At the receiver, the parameter Ns is chosen as five,000 and rate fs is ready to 500 kHz, that is that the most supported by the DAQ device. The AJSCC-encoded signal is recovered from the frequency values mistreatment straightforward linear mapping (as drained the transmitter board). The AJSCC-encoded voltage is then decoded to individual physiological and microfluidic signals mistreatment straightforward modulo arithmetic [21]. The decoded microfluidic signal in LabView is shown in Fig. 3(b) (top). It may be ascertained that the peaks of the signal are recovered. The error at the underside of the signal is due to the bias within the AJSCC stage mapping. The decoded physiological signal is shown in Fig. 3(c) (top). The division impact of the recovered physiological signal is thanks to the very fact that in the transmitter board solely eleven stages are designed for the AJSCC mapping. The error floor at the underside of the microfluidic signal is removed employing a thresholding filter, wherever the brink price is set simply higher than the error floor level. The unwanted spikes within the physiological signal are ironed employing a 200-th order median filter. the underside parts of Fig. 3(b) and (c) show the results after filtering. Scaling of physiological and resistivity cytometer values is done as follows: physiological being the electrical phenomenon measurements have the target 100's of kΩ−1 below two.6 MΩ−1, which isn't appropriate price to be fed to hardware, hence we linearly scaled the physiological values to a variety from one to three V. On the opposite hand, while microfluidic values are inside acceptable voltage ranges (0–2 V), their contribution reduces significantly within the AJSCC encoded signal thanks to 1:5 Voltage Controlled Voltage supply (VCVS) mapping within the AJSCC coding method [21]. thus we tend to had to upmarket the microfluidic signal to 0–10 V to create the microfluidic signal and its peaks apparent within the AJSCC encoded signal. within the experiments, the NI DAQ device was sampling the received baseband signal at 500 kHz; but, the Ni LabView wasn't ready to method the data at the identical rate. Hence, we tend to collected the samples alone in the LabView (without more processing) and so processed the samples in MATLAB for frequency detection and AJSCCalog domain.

B. Simulations of design 2:

In this segment, we tend to 1st concisely gift the simulation results of the improved AJSCC secret writing circuit (Design a pair of, Section II-B). Then the planned wireless biosensor system Design a pair of that enables an outsized variety of AJSCC levels is evaluated in terms of the wireless channel conditions via wireless link simulations Improved AJSCC Circuit (Design 2): Figure four shows LT Spice simulation output of the improved AJSCC circuit's output voltage (AJSCC encoded voltage) whereas varied x2 and fixing x1at 2.5 V in order that the mapped purpose can perpetually be at the middle of every level. The figure shows all the sixteen levels doable with k = four and matches the expectations of the circuit in that— we can notice a discretization within the AJSCC encoded voltage, xAJSCC attributable to the discretization of x2 by the AJSCC coding circuit. However, the quantity of discretization depends on variety the amount the quantity} of AJSCC levels and style a pair of allows the belief of an outsized number of levels simply as compared to Design one (the result shown here is specifically for sixteen levels). We describe the setup used for wireless link simulations of our wireless biosensor system with the versatile variety of AJSCC levels (i.e., adopting style 2). Wireless Link Simulation Setup: a similar cytometry and GSR information employed in the hardware experiments (Section III-A) is adopted within the wireless link machine for evaluating the system performance. The cytometry and galvanic skin response information each have sample spacing of one ms. The AJSCC encoder within the machine has the same voltage vary for x1 and x2 because the hardware PCB board, i.e., the x1 includes a most of two.25 V, and x2 includes a most of 3.0 V. the primary step is to regulate the vary of input signals, x1, x2 to the AJSCC encoder. this can be finished a linear scaling of the input signals to the input vary of AJSCC encoder. We have additionally enforced the FM adopted within the hardware board within the transmitter of wireless link machine. In the receiver, the sampled information is distributed to the FFT block for peak detection and signal recovery. 2 sets of rate and FFT sizes square measure adopted within the simulation. the primary set is that the same set of parameters employed in the hardware experiment–500 kHz sampling rate and FFT size of 5000. However, this set of parameters can need a time period of 10ms to gather the information for manufacturing one sample of the supply signal. the five hundred kHz rate in the hardware experiment is thanks to the limitation of sampling rate within the nickel DAQ device adopted within the experiment. In the simulation, we tend to square measure able to appraise at a way higher sampling rate for period of time sensing and process of the supply signal.

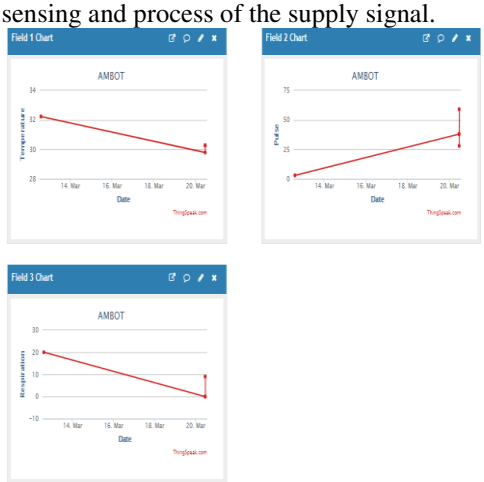

The second set of parameters is actuated from this objective. This set of parameters is meant to enhance the previous time

duration to one ms. The rate is eight.192 MHz, and therefore the FFT size is 8192. The frequency-modulated signal is mapped to frequency up to four megacycles. during this simulation, the receiver is in a position to decode the transmitted signal in real time reminiscent of the software-based style of associate degree improved digital receiver. In the receiver, the analog signal is first down converted to baseband frequency so sampled exploitation AN ADC. The digital signal is then passed to the FFT block for generating the frequency-domain response. Peak detection is after performed to search out the frequency-modulated signal to recover the AJSCC-encoded signal. The AJSCC cryptography is then performed by reverse mapping on the AJSCC curve to recover the two original mapped supply signals. On the selection of the rate, we've got evaluated 2 systems with sampling rates of five hundred kHz and eight.192 megacycles parenthetically the distinction within the performance. we are able to observe that the rate of eight.192 MHz achieves higher Mean Sq. Error (MSE) performance compared to a rate of five hundred kHz, beneath identical simulation assumptions.

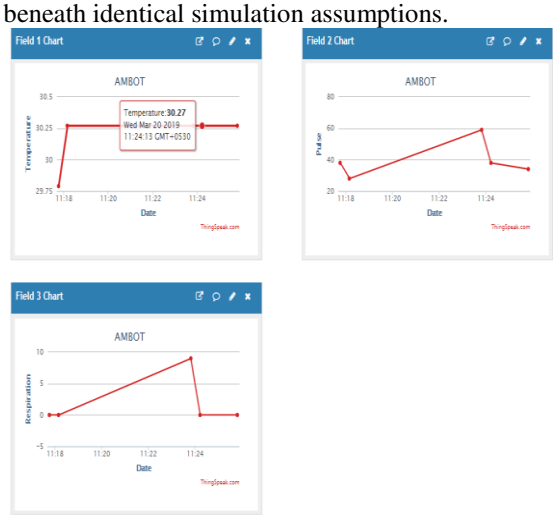

The channel modeling is crucial within the analysis of wireless system link-level performance [35], [36]. Four forms of wireless channels square measure complete within the simulator: i) Additive White Gaussian Noise (AWGN) channel; ii) Flat attenuation channel with single-tap and physicist attenuation, for modeling isotropic scattering round the receiver. there's no Christian Johann Doppler in these channel models; iii) Indoor multipath attenuation channel with Christian Johann Doppler. The channel is called JTC Indoor Residential A. JTC, that stands for Joint Technical Committee, is that the name of the multipath profile channel models [37]. This channel is nearly flat in our system and simulation setup; iv) outside multipath attenuation channel with Christian Johann Doppler twenty cycle per second. The channel model is called JTC outside Residential Areas–Low antenna A. The Christian Johann Doppler unfold is assumed as twenty cycle per second. the explanation to decide on these channel models is that our hardware experimental system is made with a pair of.4 giga cycle per second radios and works in a setting the same as Wireless native space Network (WLAN) system, that JTC channel models have been designed. A parameter named Channel signal/noise Ratio (CSNR) is outlined for evaluating the result of noise. It is defined because the quantitative relation of channel gain with signal power, to the noise variance in sound unit. Cytometry Pulse Peaks at supply and Receiver: The cytometry and psychogalvanic response supply signals square measure inputs to the AJSCC encoder in the machine. Figure five plots accumulative Distribution Function (CDF) of pulse peak values of the cytometry signal for the following cases–(i) at source; (ii) at the receiver once AJSCC decryption for AWGN channel and flat attenuation channel. The CSNR of the AWGN channel and flat attenuation channel ar all zero dB; (iii) at the receiver once AJSCC decryption for indoor channel with five cycles/second Christian Johann physicist and out of doors channel with twenty cycles/second Doppler. The CSNR of the indoor and out of doors channels ar all ten decibel for these distributions. The digital receivers of all channel conditions evaluated adopt eight.192 rate oftenness with 8192 FFT size. To quantify the similarity of the distributions between the supply and received peak values, an applied math takes a look at is necessary. The received peak information is often evaluated by the Two sample Kolmogorov-Smirnov (K-S) take a look at. The K-S take a look at is run on the two sets of knowledge, the supply cytometry peak values, and the received cytometry peak values. The digital receivers evaluated have 8.192 rate oftenness with 8192 FFT size for all channel conditions. The results of p-values at totally different AJSCC levels and therefore the K-S take a look at results ar summarized in Table I. The AWGN and flat-fading channels have zero decibel CSNR, and therefore the indoor and out of doors channels have ten decibel CSNR. From the table, we can observe that the p-values for all the channel conditions are not tiny, that indicates that there's no applied math significance to the distinction between the distributions at transmitter and receiver for all the channel conditions evaluated.

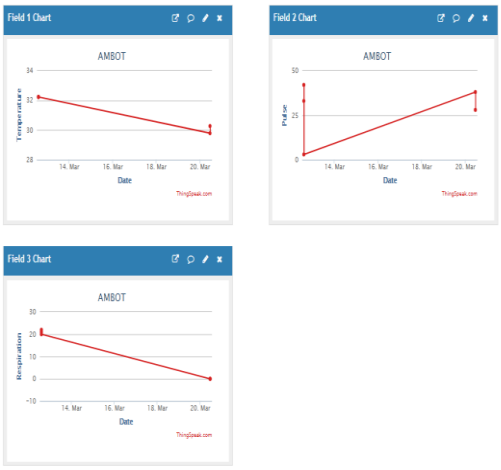

Signal Recovery Performance of AJSCC: MSE performance of the AJSCC is currently bestowed for the planned system with cytometry and galvanic skin response information as supply signals. AWGN, flat attenuation, indoor, and out of doors JTC channels ar thought-about. Performance below AWGN and Flat Attenuation Channels: The simulation results of MSE vs. the amount of parallel lines in AWGN channel ar represented in Fig. 6(a), (b). The channel has CSNR equaling to zero decibel. 2 kinds of digital receivers are evaluated—8.192 rate with 8192 FFT size (Fig. 6(b)) and five hundred kilocycle rate with 5000 FFT size (Fig. 6(a)). It is often determined that the cytometry recovery MSE performance for eight.192 rate is way lower for a number of AJSCC lines but or capable twenty compared with five hundred kilocycle rate. additionally, to data processing, this MSE advantage is that the second reason that the eight.192 MHz sampling-rate system is most popular over the five hundred kilocycle sampling rate system. The results of MSE vs. the amount of parallel lines in AJSCC for flat-fading channel with zero Christian Johann Doppler is represented in Fig. 6(c). The results of flat-fading channel ar on eight.192 MHz sampling rate system and CSNR equalling to zero decibel. we tend to observe a trade-off between the MSE of cytometry knowledge and also the electrical skin response signal altogether plots in Fig. 6. Since

the frequency information measure allotted is fixed, with increasing range of AJSCC levels, the frequency resource allotted per level is reduced, so the MSE of cytometry knowledge will increase with the rise within the range of AJSCC levels; at identical time, with such increase, the accuracy within the quantization of electrical skin response signal is improved and also the MSE of the electrical skin response signal reduces. From the curves, we will confirm the optimum number of levels in AJSCC that minimizes the add MSE, which is a sizable amount and thence is realised via style a pair of. We notice that the optimum range of levels depends on channel conditions, supply distribution, and transceiver specifications. We can also observe that the rate of eight.192 megacycle achieves better MSE performance compared with the rate of 500 kHz, underneath identical simulation assumptions. Therefore, in the following simulation evaluations of indoor and outside channels, only 8.192 megacycle rate is zero dB CSNR is depicted in Fig. 7(a), and also the result for outside channel with 20 cps Doppler and zero dB CSNR is pictured in Fig. 7(b). With higher CSNR of ten dB, the results of outside channel with twenty cps evaluated. Performance underneath Indoor and outside weakening Channels with Doppler: The results of MSE vs. the quantity of parallel lines in AJSCC for indoor and outside weakening channels (with same channel models as before) area unit evaluated. All the digital receivers have eight.192 megacycle rate and 8192 FFT size. The result for indoor channel with five cps Doppler and Doppler is pictured in Fig. 7(c). The results of indoor channel with ten dB CSNR is nearly identical to the results of ten dB CSNR of outdoor channel, thence it's not pictured. From these results, we can observe similar trade-off in MSE of the 2 supply signals for various channel conditions and receiver configurations. These results indicate the optimum range of AJSCC levels for every of the channel conditions simulated. We note that such range varies with channel conditions and transceiver parameters.

IV. CONCLUSION

We conferred a brand new style of wireless biosensing platform to measure molecular biomarkers and physiological signals at the same time, and incontestable the feasibleness of constructing this wireless biosensor. we have a tendency to mentioned and compared 2 styles for the AJSCC coding circuits. The second style provides a much higher flexibility in dominant the amount of AJSCC levels and conjointly achieves higher performance compared with the primary style. The conferred biosensor system has been evaluated via each hardware experiments additionally as wireless link simulations. Future work can embody developing a classifier on the digital receiver to classify the cells supported resistivity pulse + signals thus on estimate multiple biomarker concentrations.

ACKNOWLEDGMENT

The authors would really like to give thanks Niloy Talukder for planning the lock-in electronic equipment within the microfluidic system, and Ajinkya Padwad, Karan Ahuja, Nikitha Maiya, and Anthony rule for helping in experiments.

V. REFERENCES

[1]. X. Zhao, V. Sadhu, T. Le, M. Javanmard, and D. Pompili, "Towards low-power wearable wireless sensors for molecular biomarker and physiological signal monitoring," in Proc. IEEE Int. Symp. Circuits Syst., May 2017, pp. 1–4.

[2]. P. J. Soh, G. A. E. Vandenbosch, M. Mercuri, and D. M. M. P. Schreurs, "Wearable wireless health monitoring: Current developments, challenges, and future trends," IEEE Microw. Mag., vol. 16, no. 4, pp. 55–70, May 2015.

[3]. V. Rajendra and O. Dehzangi, "Detection of distraction under naturalistic driving using galvanic skin responses," in Proc. IEEE 14th Int. Conf. Wearable Implantable Body Sensor Netw., May 2017, pp. 157–160.

[4]. J. C. Yeo, Kenry, and C. T. Lim, "Emergence of microfluidic wearable technologies," Lab Chip, vol. 16, pp. 4082–4090, 2016. [Online]. Available: http: //dx. doi. org/ 10. 1039/C6LC00926C

[5]. A. Sun, A. G. Venkatesh, and D. A. Hall, "A multi-technique reconfigurable electrochemical biosensor: Enabling personal health monitoring in mobile devices," IEEE Trans. Biomed. Circuits Syst., vol. 10, no. 5, pp. 945–954, Oct. 2016.

[6]. S. Emaminejad, M. Javanmard, R. W. Dutton, and R. W. Davis, "Microfluidic diagnostic tool for the developing world: Contactless impedance flow cytometry," Lab Chip, vol. 12, pp. 4499–4507, 2012. [Online]. Available: http://dx. doi.org/10. 1039/C2LC40759K

[7]. R. S. Gaster et al., "Matrix-insensitive protein assays push the limits of biosensors in medicine," Nature Med., vol. 15, no. 11, pp. 1327–1332, Nov. 2009.

[8]. W. Gao et al., "Fully integrated wearable sensor arrays for multiplexed in situ perspiration analysis," Nature, vol. 529, no. 7587, pp. 509–514, Jan 2016, letter. [9] A. Gholizadeh et al., "Toward point-of-care management of chronic respiratory conditions: Electrochemical sensing of nitrite content in exhaled breath condensate using reduced graphene oxide," Microsyst. Nanoeng., vol. 3, pp. 17 022, pp. 1–8, May 2017.

[10]. Z. Lin, X. Cao, P. Xie, M. Liu, and M. Javanmard, "Picomolar level detection of protein biomarkers based on electronic sizing of bead aggregates: Theoretical and experimental considerations," Biomed. Microdevices, vol. 17, no. 6, pp. 1–7, 2015.

[11]. J. Mok, M. N. Mindrinos, R. W. Davis, and M. Javanmard, "Digital microfluidic assay for protein detection," Proc. Nat. Acad. Sci., vol. 111, no. 6, pp. 2110–2115, 2014.

[12]. M. Javanmard and R. Davis, "A microfluidic platform for electrical detection of DNA hybridization," Sens. Actuators B, Chem., vol. 154, no. 1, pp. 22–27, 2011.

[13]. N. Talukder et al., "A portable battery powered microfluidic impedance cytometer with smartphone readout: Towards personal health monitoring," Biomed. Microdevices, vol. 19, no. 2, pp. 1–15, Apr. 2017.

[14]. K. Kario et al., "Development of a new ICT-based multisensor bloodpressure monitoring system for use in hemodynamic biomarker-initiated anticipation medicine for cardiovascular disease: The national impact program project," Progress Cardiovasc. Diseases, Dec. 2017.

[15]. J. Hu et al., "Portable microfluidic and smartphone-based devices for monitoring of cardiovascular diseases at the point of care," Biotechnol. Adv., vol. 34, no. 3, pp. 305–320, 2016.

[16]. S. Imani et al., "A wearable chemical-lectrophysiological hybrid biosensing system for real-time health and fitness monitoring," Nature Commun., vol. 7, pp. 1–7, May 2016.

[17]. A. von Luhmann, H. Wabnitz, T. Sander, and K. R. Muller, "M3BA: A mobile, modular, multimodal biosignal acquisition architecture for miniaturized eeg-nirs based hybrid bci and monitoring," IEEE Trans. Biomed. Eng., vol. 64, no. 6, pp. 1199–1210, Jun. 2016.

[18]. M. A. Abrar, Y. Dong, P. K. Lee, and W. S. Kim, "Bendable electrochemical lactate sensor printed with silver nano-particles," Scientific Rep., vol. 6, pp. 1–9, Jul. 2016.

[19]. A. Nemiroski et al., "Universal mobile electrochemical detector designed for use in resource-limited applications," Proc. Nat. Acad. Sci., vol. 111, no. 33, pp. 11 984–11 989, 2014.

[20]. X. Zhao, V. Sadhu, A. Yang, and D. Pompili, "Improved circuit design of analog joint source channel coding for low-power and low-complexity wireless sensors," IEEE Sensors J., vol. 18, no. 1, pp. 281–289, Jan. 2018.

[21]. X. Zhao, V. Sadhu, and D. Pompili, "Low-power all-analog circuit for rectangular-type analog joint source channel coding," in Proc. IEEE Int. Symp. Circuits Syst., May 2016, pp. 1410–1413.

[22]. V. Sadhu, X. Zhao, and D. Pompili, "Energy-efficient analog sensing for large-scale, high-density persistent wireless monitoring," in Proc. IEEE 13th Annu. Conf. Wireless On-Demand Netw. Syst. Services, Feb. 2017, pp. 1–8.

[23]. X. Zhao, V. Sadhu, and D. Pompili, "Analog signal compression and multiplexing techniques for healthcare internet of things," in Proc. IEEE 14th Int. Conf. Mobile Ad Hoc Sensor Syst., Oct. 2017, pp. 398–406.

[24]. S. Emaminejad, M. Javanmard, R. W. Dutton, and R. W. Davis, "Microfluidic diagnostic tool for the developing world: Contactless impedance flow cytometry," Lab Chip, vol. 12, pp. 4499–4507, 2012.

[25]. K. R. Balakrishnan, G. Anwar, M. R. Chapman, T. Nguyen, A. Kesavaraju, and L. L. Sohn, "Node-pore sensing: A robust, high-dynamic range method for detecting biological species," Lab Chip, vol. 13, no. 7, pp. 1302–1307, 2013.

[26]. T. Le, G. Salles-Loustau, L. Najafizadeh, M. Javanmard, and S. Zonouz, "Biomems-based coding for secure medical diagnostic devices," in Proc. IEEE 38th Annu. Conf. Eng. Med. Biol. Soc., 2016, pp. 4419–4422.

[27]. Y. Xia and G. M. Whitesides, "Soft lithography," Annu. Rev. Mater. Sci., vol. 28, no. 1, pp. 153–184, 1998.

[28]. D. C. Duffy, J. C. McDonald, O. J. Schueller, and G. M. Whitesides, "Rapid prototyping of microfluidic systems in poly (dimethylsiloxane)," Analytical Chem., vol. 70, no. 23, pp. 4974–4984, 1998.

[29]. S. H. Tan, N.-T. Nguyen, Y. C. Chua, and T. G. Kang, "Oxygen plasma treatment for reducing hydrophobicity of a sealed polydimethylsiloxaneMicrochannel," Biomicrofluidics, vol. 4, no. 3, pp. 1–8, 2010.

[30]. W. S. Y. Libin and M. Steyaert, "A 0.8V 8 μW CMOS OTA with 50- dB gain and 1.2-MHz GBW in 18-pF load," Proc. 29th Eur. Solid-State Circuits Conf., Jun. 2003, pp. 297–300.

[31]. A. Valaee and M. Maymandi-Nejad, "An ultra-low-power low-voltage track and latch comparator," in Proc. IEEE Int. Conf. Electronics, Circuits, Syst., Dec. 2010, pp. 186–189.

[32]. Sizing Up Discrete Devices Against Integrated Circuits, 2016. [Online]. Available: http://www.mwrf.com/analog-semiconductors/sizing-discretedevices-again st-integrated-circuits

[33]. WSN430 Open Node, 2018. [online]. Available: https: //www. iot-lab.info/ hardware/wsn430/

[34]. MoteIV Telos (RevB) Low Power Wireless Sensor Module, 2004. [Online]. Available: http:// www. memsic. com/ userfiles/files/Datasheets/ WSN/telosb_datasheet.pdf

[35]. X. Zhao, R. S. K. Cheng, and D. C. Y. Ong, "A comparative analysis of pilot placement schemes in frequency-selective fast fading MIMO channel," in Proc. Wireless Telecommun. Symp., Apr. 2007, pp. 1–7.

[36]. X. Zhao, D. C. K. Lee, Z. Pan, N. Boubaker, and R. S. K. Cheng, "Modified antenna effective gain in multiple-cluster 3D channel model," in Proc. IEEE Sarnoff Symp., Apr. 2007, pp. 1–5.

[37]. M. H. Ali, A. S. Parker, and K. Pahlavan, "Frequency domain model for standard simulation of wideband radio propagation for personal communications," Electron. Lett., vol. 30, no. 25, pp. 2103–2104, Dec. 1994.

ACKNOWLEDGMENT

Xueyuan Zhao received the bachelor's and master's degrees from the Beijing University of Posts and Telecommunications (BUPT), Beijing, China. He is currently working toward the Ph.D. degree with the Electrical and Computer Engineering Department, Rutgers University, New Brunswick, NJ, USA. He is a member of the Cyber-Physical Systems Laboratory directed by Dr. D. Pompili since 2013. He worked in industry after graduation from BUPT, and contributed to multiple research and development projects. He is an inventor and co-inventor of a number of U.S. patents. He was a co-recipient of the Qualcomm Innovation Fellowship Finalist Award. 470 IEEE TRANSACTIONS ON BIOMEDICAL CIRCUITS AND SYSTEMS, VOL. 12, NO. 3, JUNE 2018

Vidyasagar Sadhu (S'17) received the B.Tech. and M.Tech. degrees (under dual degree program) in Electronics and Communications Engineering from the Indian Institute of Technology, Chennai, India, in 2012. He worked in industry for two years before joining the Ph.D. Program in Cyber Physical Systems Laboratory led by Dr. D. Pompili with the Department of Computer Engineering, Rutgers University, in 2014. His research interests are in the domain of distributed computing and machine learning, mobile phone sensing, planning under uncertainty, and wireless sensor networks. He has contributed to several research projects, a corecipient of the NSF Student Research Grant Award and the Qualcomm Innovation Fellowship Finalist Award.

Tuan Le received the B.Sc. degree in electrical and computer engineering from Rutgers University, New Brunswick, NJ, USA, in 2012, where he is currently working toward the Ph.D.

degree with NanoBioelectronics Laboratory. He joined Teletronics Technology Corporation for the duration of one and a half years as a Support Engineer. His work function included RF radio system for high-speed communication and aircraft test instrumentation. His research interests include biosensors and security for point-of-care diagnostic devices.

Dario Pompili received the Laurea (combined B.S. and M.S.) and Doctorate degrees in telecommunications and system engineering from the University of Rome La Sapienza, Rome, Italy, in 2001 and 2004, respectively, and the Ph.D. degree in electrical and computer engineering from the Georgia Institute of Technology, Atlanta, GA, USA, in 2007. He is currently an Associate Professor with the Department of electrical and computer engineering, Rutgers University, New Brunswick, NJ, USA. He is the Director of the Cyber-Physical Systems Laboratory, which focuses on mobile computing, wireless communications and networking, acoustic communications, sensor networks, and datacenter management. He was a recipient of the NSF CAREER'11, ONR Young Investigator Program'12, and DARPA Young Faculty'12 awards. In 2015, he was a nominated Rutgers' New Brunswick Chancellor's Scholar. He has published more than 100 refereed scholar publications: with over 7000 citations, he has an h-index of 31 and an i10-index of 63 (Google Scholar, in April 2018). He is a Senior Member of the IEEE Communications Society and the ACM.

Mehdi Javanmard received the B.S. degree from the Georgia Institute of Technology, in 2002, the M.S. degree in electrical engineering from Stanford University, Stanford, CA, USA, in 2004, working at Stanford Linear Accelerator Center researching the use of photonic nanostructures for high energy physics., and the Ph.D. degree in electrical engineering from Stanford University, in 2008, working on development of electronic microfluidic platforms for low-cost genomic and proteomic biomarker detection. He joined the Electrical and Computer Engineering Department, Rutgers University in Fall 2014 as an Assistant Professor. Before that, he was Senior Research Engineer at the Stanford Genome Technology Center (SGTC), School of Medicine, Stanford University. At SGTC, he worked as a postdoctoral scholar from 2008–2009, and then, as a Staff Engineering Research Associate from 2009 till 2014. His research interests include developing portable and wearable technologies for continuous health monitoring and understanding the effects of environment on health. In 2017, he was recipient of the Translational Medicine and Therapeutics Award by the American Society for Clinical Pharmacology & Therapeutics for his group's work in point of care diagnostic tools for assessing patient response to cancer therapies. He has received various awards as a Principal Investigator from the National Science Foundation, DARPA, and the PhRMA foundation to support his re